bioRxiv preprint doi: https://doi.org/10.1101/093252; this version posted December 13, 2016. The copyright holder for this preprint (which was not certified by peer review) is the author/funder, who has granted bioRxiv a license to display the preprint in perpetuity. It is made available under aCC-BY-NC 4.0 International license.

The *sek-1* p38 MAP kinase pathway regulates Gq signaling in *C. elegans*

Jill M. Hoyt, Samuel K. Wilson, Madhuri Kasa, Jeremy S. Rise,

Irini Topalidou, Michael Ailion

Department of Biochemistry, University of Washington, Seattle, WA, 98195

bioRxiv preprint doi: https://doi.org/10.1101/093252; this version posted December 13, 2016. The copyright holder for this preprint (which was not certified by peer review) is the author/funder, who has granted bioRxiv a license to display the preprint in perpetuity. It is made available under aCC-BY-NC 4.0 International license.

Running Title: *sek-1* regulates Gq signaling

key words: p38 MAPK pathway, Gq signaling, animal behavior, *C. elegans*

Corresponding author:
Michael Ailion
Department of Biochemistry
University of Washington
Box 357350
1705 NE Pacific St
Seattle, WA 98195
Phone: 206-685-0111
email: mailion@uw.edu

bioRxiv preprint doi: https://doi.org/10.1101/093252; this version posted December 13, 2016. The copyright holder for this preprint (which was not certified by peer review) is the author/funder, who has granted bioRxiv a license to display the preprint in perpetuity. It is made available under aCC-BY-NC 4.0 International license.

Abstract

Gq is a heterotrimeric G protein that is widely expressed in neurons and regulates neuronal activity. To identify pathways regulating neuronal Gq signaling we performed a forward genetic screen in *Caenorhabditis elegans* for suppressors of activated Gq. One of the suppressors is an allele of *sek-1*, which encodes a mitogen-activated protein kinase kinase (MAPKK) in the p38 MAPK pathway. Here we show that *sek-1* mutants have a slow locomotion rate and that *sek-1* acts in acetylcholine neurons to regulate both locomotion and Gq signaling. Furthermore, we find that *sek-1* acts in mature neurons to regulate locomotion. Using genetic and behavioral approaches we demonstrate that other components of the p38 MAPK pathway also play a positive role in regulating locomotion and Gq signaling. Finally, we find that mutants in the *sek-1* p38 MAPK pathway partially suppress an activated mutant of the sodium leak channel NCA-1/NALCN, a downstream target of Gq signaling. Our results suggest that the *sek-1* p38 pathway may modulate the output of Gq signaling through NCA-1.

bioRxiv preprint doi: https://doi.org/10.1101/093252; this version posted December 13, 2016. The copyright holder for this preprint (which was not certified by peer review) is the author/funder, who has granted bioRxiv a license to display the preprint in perpetuity. It is made available under aCC-BY-NC 4.0 International license.

Introduction

Gq is a widely expressed heterotrimeric G protein that regulates a variety of biological processes ranging from neurotransmission to cardiovascular pathophysiology (Sánchez-Fernández et al., 2014). In the canonical Gq pathway, Gq activates phospholipase Cβ (PLCβ), which cleaves phosphatidylinositol 4,5-bisphosphate (PIP_2) into the second messengers diacylglycerol (DAG) and inositol trisphosphate (IP_3) (Rhee, 2001). In addition to PLCβ, other Gq effectors have been identified including kinases, such as protein kinase Cζ (PKCζ) and Bruton's tyrosine kinase (Btk) (Bence et al., 1997; García-Hoz et al., 2010), and guanine nucleotide exchange factors (GEFs) for the small GTPase Rho, such as Trio (Williams et al., 2007; Vaqué et al., 2013). These noncanonical effectors bridge the activation of Gq to other cellular signaling cascades.

In order to study noncanonical pathways downstream of Gq, we used the nematode *C. elegans* which has a single Gαq homolog (EGL-30) and conservation of the other components of the Gq signaling pathway (Koelle, 2016). In neurons, EGL-30 signals through EGL-8 (PLCβ) (Lackner et al., 1999) and UNC-73 (ortholog of Trio RhoGEF) (Williams et al., 2007). UNC-73 activates RHO-1 (ortholog of RhoA), which has been shown to enhance neurotransmitter release through both diacylglycerol kinase (DGK-1)-dependent and DGK-1-independent pathways (McMullan et al., 2006).

To identify additional signaling pathways that modulate Gq signaling, we screened for suppressors of the activated Gq mutant *egl-30(tg26)* (Doi and Iwasaki, 2002), hereafter referred to as *egl-30(gf). egl-30(gf)* mutant animals exhibit hyperactive locomotion and a "loopy" posture in which worms have exaggerated, deep body bends and loop onto themselves (Bastiani et al., 2003). Here we identify one of the

bioRxiv preprint doi: https://doi.org/10.1101/093252; this version posted December 13, 2016. The copyright holder for this preprint (which was not certified by peer review) is the author/funder, who has granted bioRxiv a license to display the preprint in perpetuity. It is made available under aCC-BY-NC 4.0 International license.

suppressors as a deletion allele in the gene *sek-1*. SEK-1 is a mitogen-activated protein kinase kinase (MAPKK), the *C. elegans* ortholog of mammalian MKK3/6 in the p38 MAPK pathway (Tanaka-Hino et al., 2002). The p38 MAPK pathway has been best characterized as a pathway activated by a variety of cellular stresses and inflammatory cytokines (Kyriakis and Avruch, 2012). However, the p38 MAPK pathway has also been shown to be activated downstream of a G protein-coupled receptor in rat neurons (Huang et al., 2004). Btk, a member of the Tec family of tyrosine kinases, has been shown to act downstream of Gq to activate the p38 MAPK pathway (Bence et al., 1997), but *C. elegans* lacks Btk and other Tec family members (Plowman et al., 1999).

SEK-1 is activated by the MAPKKK NSY-1 (ortholog of ASK1) and activates the p38 MAPKs PMK-1 and PMK-2 (Andrusiak and Jin, 2016). The p38 MAPK pathway consisting of NSY-1/SEK-1/PMK-1 is required for innate immunity in *C. elegans* (Kim et al., 2002). NSY-1 and SEK-1 are also required for the specification of the asymmetric AWC olfactory neurons (Sagasti et al., 2001; Tanaka-Hino et al., 2002); the p38 orthologs PMK-1 and PMK-2 function redundantly in AWC specification (Pagano et al., 2015). For both innate immunity and AWC specification, the p38 MAPK pathway acts downstream of the adaptor protein TIR-1 (an ortholog of SARM) (Couillault et al., 2004; Chuang and Bargmann, 2005). Here we show that the TIR-1/NSY-1/SEK-1/PMK-1 PMK-2 signaling module also acts to regulate locomotion downstream of Gq signaling.

Materials and Methods

C. elegans strains and maintenance

bioRxiv preprint doi: https://doi.org/10.1101/093252; this version posted December 13, 2016. The copyright holder for this preprint (which was not certified by peer review) is the author/funder, who has granted bioRxiv a license to display the preprint in perpetuity. It is made available under aCC-BY-NC 4.0 International license.

All strains were cultured using standard methods and maintained at 20°C (Brenner, 1974). The *sek-1(yak42)* mutant was isolated from an ENU mutagenesis suppressor screen of the activated Gq mutant *egl-30(tg26)* ("*egl-30(gf)*") (Ailion et al., 2014). *sek-1(yak42)* was outcrossed away from *egl-30(gf)* before further analysis. Double mutant strains were constructed using standard methods (Fay, 2006) often with linked fluorescent markers (Frokjaer-Jensen et al., 2014) to balance mutations with subtle visible phenotypes. Table S1 contains all the strains used in this study.

Mapping

yak42 was mapped using the slow locomotion phenotype and its *egl-30(gf)* suppression phenotype. *yak42* was initially mapped to Chromosome X using strains EG1000 and EG1020, which carry visible marker mutations. These experiments showed that *yak42* was linked to *lon-2*, but at least several map units away. *yak42* was further mapped to about one map unit (m.u.) away from the red fluorescent insertion marker *oxTi668* which is located at +0.19 m.u. on Chromosome X.

Whole-genome sequencing

Strain XZ1233 *egl-30(tg26); yak42* was used for whole-genome sequencing to identify candidate *yak42* mutations. XZ1233 was constructed by crossing a 2X outcrossed *yak42* strain back to *egl-30(tg26)*. Thus, in XZ1233, *yak42* has been outcrossed 3X from its original isolate. DNA was isolated from XZ1233 and purified according to the Hobert Lab protocol (http://hobertlab.org/whole-genome-sequencing/). Ion Torrent sequencing was performed at the University of Utah DNA Sequencing Core

bioRxiv preprint doi: https://doi.org/10.1101/093252; this version posted December 13, 2016. The copyright holder for this preprint (which was not certified by peer review) is the author/funder, who has granted bioRxiv a license to display the preprint in perpetuity. It is made available under aCC-BY-NC 4.0 International license.

Facility. The resulting data contained 10,063,209 reads of a mean read length of 144 bases, resulting in about 14X average coverage of the *C. elegans* genome. The sequencing data were uploaded to the CloudMap pipeline on the Galaxy platform (Minevich et al., 2012) and SNPs and indels were identified. We filtered out polymorphisms found in other strains we sequenced, leaving us with 605 homozygous mutations. Chromosome X contained 94 mutations: 55 SNPs and 39 indels. Of these, four SNPs were non-synonymous mutations in protein-coding genes, but only 2 were within 5 m.u. of *oxTi668.* However, we were unable to identify *yak42* from the candidate polymorphisms located near *oxTi668*. Transgenic expression of the most promising candidate *pcyt-1* (located at -1.49 m.u.) did not rescue *yak42*. Instead, to identify possible deletions, we scrolled through 2 MB of aligned reads on the UCSC Genome Browser starting at -4.38 m.u. and working towards the middle of the chromosome (0 m.u.), looking for regions that lacked sequence coverage. We found a 3713 bp deletion that was subsequently confirmed to be the *yak42* causal mutation, affecting the gene *sek-1* located at -1.14 m.u.

Locomotion assays

Locomotion assay plates were made by seeding 10 cm nematode growth medium plates with 150 µl of an OP50 (a strain of *E. coli*) stock culture, spread with sterile glass beads to cover the entire plate. Bacterial lawns were grown at room temperature (22.5°C -24.5°C) for 24 hrs and then stored at 4°C until needed. All locomotion assays were performed on first day adults. L4 stage larvae were picked the day before the assay and the experimenter was blind to the genotypes of the strains

bioRxiv preprint doi: https://doi.org/10.1101/093252; this version posted December 13, 2016. The copyright holder for this preprint (which was not certified by peer review) is the author/funder, who has granted bioRxiv a license to display the preprint in perpetuity. It is made available under aCC-BY-NC 4.0 International license.

assayed. For experiments on strains carrying extrachromosomal arrays, the *sek-1(km4)* control worms were animals that had lost the array from the same plate.

Body bends assays were performed as described (Miller et al., 1999). The locomotion assay plate was brought to room temperature (22.5°C -24.5°C). All strains in an experiment were assayed on the same assay plate. A single animal was picked onto the plate, the plate lid was returned, and the animal recovered for 30 s. Body bends were then counted for one minute. A body bend was counted each time the worm's tail reached the minimum or maximum amplitude of the sine wave. For experiments with *egl-8*, *unc-73*, and *rund-1*, worms were allowed a minimal recovery period (until the worms started moving forward, 5 sec maximum) prior to counting body bends.

For the heat shock experiment, plates of first-day adults were parafilmed and heatshocked in a 34°C water bath for 1 hr. Plates were then un-parafilmed and incubated at 20°C for five hours before performing body bend assays.

Radial locomotion assays were performed by first bringing the locomotion assay plates to room temperature. Animals were picked to the middle of the plate, the plate taped shut, and an x was marked on the lid above where the animals were placed. Assay plates were then incubated at 20°C for 20 hr and the distances of the worms from the starting point were measured.

Quantitative analysis of the waveform of worm tracks was performed by first bringing the locomotion assay plate to room temperature. One strain at a time, five animals were placed on the plate and allowed to roam for 2-5 min. We then took five pictures of each animal's tracks following forward locomotion. Track pictures were taken at 40X on a Nikon SMZ18 microscope with the DS-L3 camera control system. This

bioRxiv preprint doi: https://doi.org/10.1101/093252; this version posted December 13, 2016. The copyright holder for this preprint (which was not certified by peer review) is the author/funder, who has granted bioRxiv a license to display the preprint in perpetuity. It is made available under aCC-BY-NC 4.0 International license.

process was repeated for all strains per experiment set. Worm track pictures were processed using ImageJ. Tracks were straightened with the segmented line tool and pictures converted to grayscale. Period and 2X amplitude were measured freehand using the line tool. For each worm, five period/amplitude ratios were calculated from each of the five straightened tracks. The ratios were averaged for each worm and these averages were averaged for each strain.

C. elegans pictures

Pictures of worms were taken at 60X on a Nikon SMZ18 microscope with the DS-L3 camera control system. The worms were age-matched as first day adults and each experiment set was photographed on the same locomotion assay plate (assay plate preparation described above). The images were processed using ImageJ and were rotated, cropped, and converted to grayscale.

Molecular biology

Plasmids were constructed using the Gateway cloning system (Invitrogen). Plasmids and primers used are found in Table S2. The *sek-1* cDNA was amplified by RT-PCR from worm RNA and cloned into a Gateway entry vector. To check for proper expression of *sek-1*, an operon GFP was included in expression constructs with the following template: (promoter)p::*sek-1*(cDNA)::*tbb-2utr::gpd-2 operon::GFP::H2B:cye-1utr* (Frøkjær-Jensen et al., 2012). This resulted in untagged SEK-1, but expression could be monitored by GFP expression.

bioRxiv preprint doi: https://doi.org/10.1101/093252; this version posted December 13, 2016. The copyright holder for this preprint (which was not certified by peer review) is the author/funder, who has granted bioRxiv a license to display the preprint in perpetuity. It is made available under aCC-BY-NC 4.0 International license.

Injections

C. elegans strains with extrachromosomal arrays were generated by standard methods (Mello et al., 1991). Injection mixes were made with a final total concentration of 100 ng/µL DNA. Constructs were injected at 5 ng/µL, injection markers at 5 ng/µL, and the carrier DNA Litmus 38i at 90 ng/µL. Multiple lines of animals carrying extrachromosomal arrays were isolated and had similar behaviors as observed by eye. The line with the highest transmittance of the array was assayed.

Statistical analysis

At the beginning of the project, a power study was conducted on pilot body bend assays using wild type and *sek-1(yak42)* worms. To achieve a power of 0.95, it was calculated that 17 animals should be assayed per experiment. Data were analyzed to check if normally distributed (using the D'Agostino-Pearson and Shapiro-Wilk normality tests) and then subjected to the appropriate analysis using GraphPad Prism 5. For data sets with three or more groups, if the data were normal they were analyzed with a one-way ANOVA; if not, with a Kruskal-Wallis test. Post-hoc tests were used to compare appropriate data sets within an experiment. Reported p-values are corrected. Table S3 contains the statistical tests for each experiment. $p<0.05$ = *; $p<0.01$ = **; $p<0.001$ = ***.

Reagent and Data Availability

Strains and plasmids are shown in Table S1 and Table S2 and are available from the *Caenorhabditis* Genetics Center (CGC) or upon request. The authors state that all

bioRxiv preprint doi: https://doi.org/10.1101/093252; this version posted December 13, 2016. The copyright holder for this preprint (which was not certified by peer review) is the author/funder, who has granted bioRxiv a license to display the preprint in perpetuity. It is made available under aCC-BY-NC 4.0 International license.

data necessary for confirming the conclusions presented in the article are represented fully within the article and Supplemental Material.

Results

sek-1 suppresses activated Gq

To identify downstream effectors of Gαq, we performed a forward genetic screen for suppressors of the activated Gq mutant, *egl-30(tg26)* (Doi and Iwasaki, 2002), referred to here as *egl-30(gf). egl-30(gf)* worms are small, hyperactive, and have a "loopy" posture characterized by a high-amplitude waveform (Figure 1B). Thus, we screened for worms that are larger, less hyperactive, and less loopy. We isolated a recessive suppressor, *yak42*, and mapped it to the middle of Chromosome X (see Materials and Methods). Whole-genome sequencing revealed that *yak42* carries a large deletion of the *sek-1* gene from upstream of the start codon to exon 4 (Figure 1A). *yak42* also failed to complement *sek-1(km4)*, a previously published *sek-1* deletion allele (Figure 1A) (Tanaka-Hino et al., 2002).

egl-30(gf) double mutants with either *sek-1(yak42)* or *sek-1(km4)* are bigger than *egl-30(gf)* worms (Figure 1B), not hyperactive (Figure 1C). and have a tendency to kink when moving backward. Additionally, both *sek-1* mutations suppress the loopy waveform phenotype (Figure S1A, B).

sek-1(yak42) was outcrossed from *egl-30(gf)* and assayed for locomotion defects. Both the *sek-1(yak42)* and *sek-1(km4)* mutants are coordinated but move more slowly than wild-type (Figure 1D). *sek-1(ag1)*, a point mutation in exon 5 (Kim et al., 2002), also causes a similar slow locomotion phenotype (Figure S1C). To test whether

bioRxiv preprint doi: https://doi.org/10.1101/093252; this version posted December 13, 2016. The copyright holder for this preprint (which was not certified by peer review) is the author/funder, who has granted bioRxiv a license to display the preprint in perpetuity. It is made available under aCC-BY-NC 4.0 International license.

the *egl-30(gf)* suppression phenotype might be an indirect effect of the slow locomotion of a *sek-1* mutant, we built an *egl-30(gf)* double mutant with a mutation in *unc-82*, a gene required for normal muscle structure. *unc-82* mutants are coordinated but move slowly, similar to a *sek-1* mutant (Hoppe et al., 2010). However, although an *egl-30(gf) unc-82(e1220)* double mutant moves more slowly than *egl-30(gf)*, it is still small and loopy (Figure 1B). Thus, *sek-1* appears to be a specific suppressor of multiple phenotypes of the *egl-30(gf)* mutant, suggesting that *sek-1* regulates locomotion and acts downstream of Gq.

EGL-30/Gαq is negatively regulated by GOA-1, the worm Gαo/i ortholog (Hajdu-Cronin et al., 1999). We tested whether *sek-1* also suppresses a *goa-1* loss-of-function mutant that causes a hyperactive phenotype similar to *egl-30(gf).* Indeed, *sek-1(km4)* suppresses *goa-1(sa734)* (Figure S1D). One downstream effector of GOA-1 is the DAG kinase DGK-1 (DGKΘ ortholog) that inhibits DAG-dependent functions such as synaptic vesicle release (Nurrish *et al.* 1999; Miller *et al.* 1999). *dgk-1(sy428)* animals are hyperactive, but *sek-1(km4)* does not suppress *dgk-1*. Rather, the *sek-1 dgk-1* double mutant is uncoordinated and looks like neither *sek-1* nor *dgk-1* mutants, confounding the interpretation of how *sek-1* genetically interacts with *dgk-1*.

sek-1 acts in mature acetylcholine neurons

egl-30 is widely expressed and acts in neurons to regulate locomotion (Lackner et al., 1999), so it is possible that *sek-1* also acts in neurons to regulate Gq signaling. *sek-1* is expressed in neurons, intestine, and several other tissues (Tanaka-Hino et al.,

bioRxiv preprint doi: https://doi.org/10.1101/093252; this version posted December 13, 2016. The copyright holder for this preprint (which was not certified by peer review) is the author/funder, who has granted bioRxiv a license to display the preprint in perpetuity. It is made available under aCC-BY-NC 4.0 International license.

2002) and has been shown to function in GABA neurons to possibly promote GABA release (Vashlishan et al., 2008).

To identify the cell type responsible for the *sek-1* locomotion phenotypes, we expressed the wild-type *sek-1* cDNA under different cell-specific promoters and tested for transgenic rescue of a *sek-1* null mutant. Expression of *sek-1* in all neurons (using the *unc-119* promoter) or in acetylcholine neurons (using *unc-17p*) was sufficient to rescue the *sek-1* mutant slow locomotion phenotype, but expression in GABA neurons (using *unc-47p*) was not sufficient to rescue (Figure 2A, B). These results indicate that *sek-1* acts in acetylcholine neurons to regulate locomotion.

We next tested whether *sek-1* also acts in neurons to suppress *egl-30(gf)*. Expression of *sek-1* under pan-neuronal and acetylcholine neuron promoters rescued the *sek-1* suppression of *egl-30(gf)*. Specifically, *egl-30(gf) sek-1* double mutants expressing wild-type *sek-1* in all neurons or acetylcholine neurons had a hyperactive, loopy, small phenotype that resembled the *egl-30(gf)* single mutant (Figure 2C, D). However, expression of *sek-1* in GABA neurons did not rescue the suppression phenotype (Figure 2C, D). Together, these data show that *sek-1* acts in acetylcholine and not GABA neurons to regulate both wild-type locomotion and to modulate Gq signaling.

Because *sek-1* acts in the development of the AWC asymmetric neurons, we asked whether *sek-1* also has a developmental role in regulating locomotion by testing whether adult-specific *sek-1* expression (driven by a heat-shock promoter) is sufficient to rescue the *sek-1* mutant. We found that *sek-1* expression in adults rescues the *sek-1* slow locomotion phenotype (Figure 2E). This result indicates that *sek-1* is not required

bioRxiv preprint doi: https://doi.org/10.1101/093252; this version posted December 13, 2016. The copyright holder for this preprint (which was not certified by peer review) is the author/funder, who has granted bioRxiv a license to display the preprint in perpetuity. It is made available under aCC-BY-NC 4.0 International license.

for development of the locomotion circuit and instead acts in mature neurons to regulate locomotion.

The p38 MAPK pathway is a positive regulator of Gq signaling

SEK-1 is the MAPKK in a p38 MAPK pathway (Tanaka-Hino et al., 2002). This pathway consists of NSY-1 (MAPKKK), SEK-1 (MAPKK), and PMK-1 or PMK-2 (MAPKs)(Andrusiak and Jin, 2016). TIR-1 acts upstream of NSY-1. This p38 MAPK signaling module has been shown to function in innate immunity and the development of the AWC olfactory neurons (Chuang and Bargmann, 2005).

We tested whether the entire p38 MAPK and TIR-1 signaling module also regulates locomotion and suppression of activated Gq. Both *tir-1(tm3036)* and *nsy-1(ok593)* mutant animals have slow locomotion on their own and also suppress the hyperactivity, deep body bends and small size of *egl-30(gf)* (Figure 3A-D; Figure S2A, B). We also tested single mutants in each of the three worm p38 MAPK genes (*pmk-1, pmk-2* and *pmk-3)* and a *pmk-2 pmk-1* double mutant. Although we found that the *pmk-2* and *pmk-3* single mutants were slightly slow on their own, only the *pmk-2 pmk-1* double mutant phenocopied *sek-1* and suppressed both the hyperactivity and deep body bends of *egl-30(gf)* (Figure 3, E-G). Thus, *pmk-2* and *pmk-1* act redundantly downstream of *sek-1* to suppress *egl-30(gf).* These data suggest that the p38 MAPK pathway regulates locomotion in *C. elegans* and acts genetically downstream of *egl-30*.

The JNK MAPK pathway, related to the p38 MAPK family, also regulates locomotion in *C. elegans*. Specifically, the JNK pathway members *jkk-1* (JNK MAPKK) and *jnk-1* (JNK MAPK) have been shown to act in GABA neurons to regulate

bioRxiv preprint doi: https://doi.org/10.1101/093252; this version posted December 13, 2016. The copyright holder for this preprint (which was not certified by peer review) is the author/funder, who has granted bioRxiv a license to display the preprint in perpetuity. It is made available under aCC-BY-NC 4.0 International license.

locomotion (Kawasaki et al., 1999). We found that the *jkk-1* and *jnk-1* single mutants had slow locomotion and that the double mutants with p38 MAPK pathway members exhibited an additive slow locomotion phenotype (Figure S2C). Moreover, neither *jkk-1* nor *jnk-1* suppressed *egl-30(gf)* (data not shown). Thus, the JNK and p38 MAPK pathways regulate locomotion independently and the JNK pathway is not involved in Gq signaling.

We also tested the involvement of possible p38 MAPK pathway effectors. One of the targets of PMK-1 is the transcription factor ATF-7 (Shivers et al., 2010). Both the *atf-7(qd22 qd130)* loss-of-function mutant and the *atf-7(qd22)* gain-of-function mutant moved slowly compared to wild-type animals (Figure S2D). However, *atf-7(qd22 qd130)* did not suppress *egl-30(gf)* (data not shown), suggesting that *atf-7* is not a target of this pathway or acts redundantly with other downstream p38 MAPK targets. We also tested *gap-2*, the closest *C. elegans* homolog of ASK1-interacting Protein (AIP1) which activates ASK1 (the ortholog of *C. elegans* NSY-1) in mammalian systems (Zhang et al., 2003). A *C. elegans gap-2* mutant has no locomotion defect (Figure S2E). Finally, we tested VHP-1, a phosphatase for p38 and JNK MAPKs that inhibits p38 MAPK signaling (Kim et al., 2004). However, the *vhp-1(sa366)* mutant also has no locomotion defect (Figure S2E).

egl-30(gf) animals are loopy and hyperactive so we tested whether increased activation of the TIR-1/p38 MAPK signaling module causes similar phenotypes. The *tir-1(ky648gf)* allele leads to a gain-of-function phenotype in the AWC neuron specification (Chang et al., 2011), but does not cause a locomotion phenotype reminiscent of *egl-30(gf)* (Figure S2F, G).

bioRxiv preprint doi: https://doi.org/10.1101/093252; this version posted December 13, 2016. The copyright holder for this preprint (which was not certified by peer review) is the author/funder, who has granted bioRxiv a license to display the preprint in perpetuity. It is made available under aCC-BY-NC 4.0 International license.

Genetic interactions of *sek-1* with pathways acting downstream of Gq

Our forward genetic screen for suppressors of *egl-30(gf)* identified mutants that fall into three different categories: mutants in the canonical Gq pathway such as the PLC *egl-8* (Lackner et al., 1999), mutants in the RhoGEF Trio pathway such as *unc-73* (Williams et al., 2007), and mutants that affect dense-core vesicle biogenesis and release (Ailion et al., 2014; Topalidou et al., 2016a).

To test if *sek-1* acts in these pathways we used genetic epistasis analysis. Loss-of-function alleles of *egl-8(sa47)*, *unc-73(ox317),* and *rund-1(tm3622)* have slow locomotion (Figure 4A-C). Our data show that *sek-1* enhances the phenotype of *egl-8* and *rund-1* single mutants, suggesting that *sek-1* does not act in the same pathway as *egl-8* or *rund-1* (Figure 4A, B). By contrast, *sek-1* does not enhance the slow locomotion phenotype of *unc-73* mutants (Figure 4C), suggesting that *sek-1* may act in the same genetic pathway as the Trio RhoGEF *unc-73.*

We next tested whether *sek-1* interacts with *rho-1*, encoding the small G protein activated by Trio. *rho-1* is required for viability so we could not use a loss-of-function allele to test for a genetic interaction (Jantsch-Plunger et al., 2000). Instead we used an integrated transgene overexpressing an activated *rho-1* mutant allele specifically in acetylcholine neurons. Animals carrying this activated RHO-1 transgene, referred to here as *rho-1(gf)*, have a loopy posture reminiscent of *egl-30(gf)* (McMullan et al., 2006), and a decreased locomotion rate. *rho-1(gf) sek-1(km4)* double mutants had a loopy body posture like *rho-1(gf)* and an even slower locomotion rate (Figure 4D, E), suggesting that *sek-1* and *rho-1(gf)* mutants have additive locomotion phenotypes.

bioRxiv preprint doi: https://doi.org/10.1101/093252; this version posted December 13, 2016. The copyright holder for this preprint (which was not certified by peer review) is the author/funder, who has granted bioRxiv a license to display the preprint in perpetuity. It is made available under aCC-BY-NC 4.0 International license.

However, both *sek-1(km4)* and *sek-1(yak42)* suppress the slow growth rate of the *rho-1(gf)* mutant. Because *sek-1* does not enhance *unc-73* mutants and suppresses some aspects of the *rho-1(gf)* mutant, *sek-1* may modulate output of the Rho pathway, though it probably is not a direct transducer of Rho signaling.

sek-1 and _nsy-1_ partially suppress activated NCA

The data above did not clarify the relationship of *sek-1* to the Rho pathway acting downstream of Gq. The downstream target of this Gq-Rho pathway appears to be the NCA-1 cation channel (Topalidou et al., 2016b). NCA-1 and its orthologs are sodium leak channels associated with rhythmic behaviors in several organisms (Nash et al., 2002; Lu et al., 2007; Shi et al., 2016). In *C. elegans*, NCA-1 potentiates persistent motor circuit activity and sustains locomotion (Gao et al., 2015).

To examine interactions of the *sek-1* p38 MAPK pathway with NCA-1, we tested whether *sek-1* and *nsy-1* mutants suppress the activated NCA-1 mutant *ox352*, referred to as *nca-1(gf)*. The *nca-1(gf)* animals are coiled and uncoordinated; thus, it is difficult to measure their locomotion rate by the body bend assay because they sometimes do not propagate sinusoidal waves down the entire length of their body. Instead, we used a radial locomotion assay in which we placed animals in the center of a 10 cm plate and later measured how far the animals had moved. *nca-1(gf)* double mutants with either *sek-1(km4)* or *nsy-1(ok593)* uncoil a bit but still exhibit uncoordinated locomotion (Figure 5A). In fact, though these double mutants show more movement in the anterior half of their bodies than *nca-1(gf)*, they propagate body waves to their posterior half even more poorly than the *nca-1(gf)* mutant. However, both *sek-1* and *nsy-1* clearly

bioRxiv preprint doi: https://doi.org/10.1101/093252; this version posted December 13, 2016. The copyright holder for this preprint (which was not certified by peer review) is the author/funder, who has granted bioRxiv a license to display the preprint in perpetuity. It is made available under aCC-BY-NC 4.0 International license.

suppress the small size and slow growth rate of the *nca-1(gf)* mutant (Figure 5A) and in radial locomotion assays, *sek-1* and *nsy-1* weakly suppressed the *nca-1(gf)* locomotion phenotype (Figure 5B). Together these data suggest that mutants in the *sek-1* p38 MAPK pathway partially suppress some aspects of the *nca-1(gf)* mutant.

Given that *sek-1* acts in acetylcholine neurons to regulate wild-type and *egl-30(gf)* locomotion, we tested if the same neuron class is responsible for *sek-1* suppression of *nca-1(gf)*. Expression of *sek-1* in all neurons or in acetylcholine neurons of *nca-1(gf) sek-1(km4)* animals restored the *nca-1(gf)* size and posture phenotypes. These worms are small and coiled and closely resemble the *nca-1(gf)* mutant (Figure 5C). By contrast, expression of *sek-1* in GABA neurons did not affect the size or posture of the *nca-1(gf) sek-1* double mutant (Figure 5C). These data suggest that *sek-1* acts in acetylcholine neurons to regulate *nca-1(gf)* locomotion. However, in radial locomotion assays, expression of *sek-1* in none of these neuron classes significantly altered the movement of the *nca-1(gf) sek-1* double mutant (Figure 5D), though the weak suppression of *nca-1(gf)* by *sek-1* in this assay makes it difficult to interpret these negative results. We make the tentative conclusion that *sek-1* partially suppresses *nca-1(gf)* locomotion and probably acts in the acetylcholine neurons where it also acts to regulate wild-type and *egl-30(gf)* locomotion, suggesting a common neuronal site of action of this pathway.

Discussion

In this study we identified a new neuronal role for the mitogen-activated protein kinase kinase SEK-1 and the p38 MAPK pathway as a positive regulator of locomotion

bioRxiv preprint doi: https://doi.org/10.1101/093252; this version posted December 13, 2016. The copyright holder for this preprint (which was not certified by peer review) is the author/funder, who has granted bioRxiv a license to display the preprint in perpetuity. It is made available under aCC-BY-NC 4.0 International license.

and Gq signaling. The p38 MAPK pathway has been best characterized as a pathway activated by a variety of cellular stresses and inflammatory cytokines (Kyriakis and Avruch, 2012), but it has also been implicated in neuronal function, including some forms of mammalian synaptic plasticity (Bolshakov *et al.* 2000; Rush *et al.* 2002; Huang *et al.* 2004). In *C. elegans*, Gq plays a positive role in locomotion by promoting acetylcholine release, so we tested whether the slow locomotion of *sek-1* mutants is directly related to the role of *sek-1* as a regulator of Gq signaling. Through rescue experiments, we found that SEK-1 acts in acetylcholine neurons to regulate both the rate of locomotion and Gq signaling. Previously, *sek-1* has been shown to act in GABA neurons to regulate sensitivity to the acetylcholinesterase inhibitor aldicarb (Vashlishan et al., 2008), and to act in interneurons to regulate trafficking of the GLR-1 glutamate receptor and the frequency of worm reversals (Park and Rongo, 2016). Thus, *sek-1* may play distinct roles in different neuron types. Our data indicate a role for *sek-1* as a positive regulator of Gq signaling in acetylcholine neurons.

In addition to SEK-1, we identified other p38 pathway components regulating Gq signaling. Specifically, we found that mutants in *tir-1*, *nsy-1* and a *pmk-1 pmk-2* double mutant exhibit locomotion defects identical to *sek-1* and suppress activated Gq, suggesting that they act in a single p38 pathway to modulate signaling downstream of Gq. These results indicate a redundant function for PMK-1 and PMK-2 in regulating locomotion rate and Gq signaling. PMK-1 and PMK-2 also act redundantly for development of the asymmetric AWC neurons and to regulate induction of serotonin biosynthesis in the ADF neurons in response to pathogenic bacteria (Pagano et al.,

bioRxiv preprint doi: https://doi.org/10.1101/093252; this version posted December 13, 2016. The copyright holder for this preprint (which was not certified by peer review) is the author/funder, who has granted bioRxiv a license to display the preprint in perpetuity. It is made available under aCC-BY-NC 4.0 International license.

2015). By contrast, PMK-1 acts alone in the intestine to regulate innate immunity and in interneurons to regulate GLR-1 trafficking (Pagano et al., 2015; Park and Rongo, 2016).

What is the downstream effector of *sek-1* p38 MAPK signaling in this Gq signaling pathway? There are several known downstream effectors of p38 MAPK signaling in *C. elegans*, including the transcription factor ATF-7 (Shivers et al., 2010; Inoue et al., 2005; Xie et al., 2013). Our data indicate that ATF-7 is not required for the p38 MAPK-dependent regulation of Gq signaling. It is possible that this p38 MAPK pathway activates molecules other than transcription factors to regulate Gq signaling. It is also possible that the *sek-1* p38 pathway activates multiple downstream effectors that are not individually required.

One of the pathways that transduce signals from Gq includes the RhoGEF Trio/UNC-73, the small GTPase Rho, and the cation channel NALCN/NCA-1 (Williams et al., 2007; Topalidou et al., 2016b). We found that mutations in the *sek-1* p38 MAPK pathway partially suppress an activated NCA-1 mutant and that *sek-1* probably acts to control NCA-1 activity in the same neurons where it acts to regulate locomotion and Gq signaling. Given the precedence for direct phosphorylation of sodium channels by p38 to regulate channel properties (Wittmack et al., 2005; Hudmon et al., 2008), it is possible that PMK-1 and PMK-2 phosphorylate NCA-1 to regulate its expression, localization, or activity. Our genetic study sets the foundation for further investigation of the specific role of the *sek-1* p38 pathway in the regulation of Gq signaling and NCA-1 channel activity.

Acknowledgements

bioRxiv preprint doi: https://doi.org/10.1101/093252; this version posted December 13, 2016. The copyright holder for this preprint (which was not certified by peer review) is the author/funder, who has granted bioRxiv a license to display the preprint in perpetuity. It is made available under aCC-BY-NC 4.0 International license.

We thank Dennis Kim and Chiou-Fen Chuang for strains, Pin-An Chen and Erik Jorgensen for the *nca-1(gf)* mutant *ox352*, Chris Johnson for the fine mapping of *yak42*, Jordan Hoyt for help with Galaxy and CloudMap to analyze WGS data, and Dana Miller for providing access to her microscope camera. Some strains were provided by the CGC, which is funded by NIH Office of Research Infrastructure Programs (P40 OD010440). J.M.H was supported in part by Public Health Service, National Research Service Award T32GM007270, from the National Institute of General Medical Sciences. M.A. is an Ellison Medical Foundation New Scholar. This work was supported by NIH grant R00 MH082109 to M.A.

Figure Legends

Figure 1: *sek-1* acts downstream of Gαq to regulate locomotion behavior

(a) Gene structure of *sek-1*. White boxes depict the 5' and 3' untranslated regions, black boxes depict exons, and lines show introns. The positions of the *yak42* and *km4* deletions are shown. *yak42* is a 3713 bp deletion that extends to 1926 bp upstream of the start codon. Drawn with Exon-Intron Graphic Maker (http://www.wormweb.org/exonintron). Scale bar is 100 bp.

(b) *sek-1(yak42)* and *sek-1(km4)* suppress the small size and loopy waveform of *egl-30(tg26)*, written here as *egl-30(gf). unc-82(e1220)* does not suppress *egl-30(gf).* Photos of first-day adult worms. WT: wild type.

(c) *egl-30(gf)* is hyperactive compared to wild-type and suppressed by *sek-1(yak42)* and *sek-1(km4)*. ***, $p<0.001$, error bars = SEM, n=20.

bioRxiv preprint doi: https://doi.org/10.1101/093252; this version posted December 13, 2016. The copyright holder for this preprint (which was not certified by peer review) is the author/funder, who has granted bioRxiv a license to display the preprint in perpetuity. It is made available under aCC-BY-NC 4.0 International license.

(d) *sek-1* mutant worms have slow locomotion. ***, p<0.001 compared to wild-type, error bars = SEM, n=20.

Figure 2: *sek-1* acts in mature acetylcholine neurons to regulate locomotion

(A) *sek-1* acts in neurons to regulate locomotion. The *sek-1* wild-type cDNA driven by the *unc-119* pan-neuronal promoter *[unc-119p::sek-1(+)]* rescues the slow locomotion phenotype of *sek-1(km4)* worms. ***, p< 0.001, error bars = SEM, n=20.

(B) *sek-1* acts in acetylcholine neurons to regulate locomotion. *sek-1* WT cDNA driven by the *unc-17* acetylcholine neuron promoter *[unc-17p::sek-1(+)]* rescues the slow locomotion phenotype of *sek-1(km4)* worms but *sek-1* expression in GABA neurons using the *unc-47* promoter *[unc-47p::sek-1(+)]* does not. p< 0.001, error bars = SEM, n=20.

(C-D) *sek-1* acts in acetylcholine neurons to suppress *egl-30(gf).* Worms expressing *unc-119p::sek-1(+)* or *unc-17p::sek-1(+)* do not have the *egl-30(gf) sek-1* phenotype but worms expressing *unc-47p::sek-1(+)* are identical to *egl-30(gf) sek-1* both for waveform (C) and in the locomotion assay (D). Kruskal-Wallis test, ***, p< 0.001, **, p<0.01; error bars = SEM, n=17-20.

(E) *sek-1* acts in mature neurons to regulate locomotion. *hsp-16.2p::sek-1(+)* rescues the slow locomotion phenotype of *sek-1(km4)*. ***, p< 0.001, error bars = SEM, n=20.

Figure 3: The p38 MAPK pathway regulates locomotion downstream of *egl-30*

(A) *tir-1(tm3036)* mutant animals have slow locomotion. ***, p<0.001, error bars = SEM, n=20.

bioRxiv preprint doi: https://doi.org/10.1101/093252; this version posted December 13, 2016. The copyright holder for this preprint (which was not certified by peer review) is the author/funder, who has granted bioRxiv a license to display the preprint in perpetuity. It is made available under aCC-BY-NC 4.0 International license.

(B) *tir-1(tm3036)* suppresses *egl-30(gf)*. *egl-30(gf) tir-1* animals move more slowly than the hyperactive *egl-30(gf)* animals. ***, p< 0.001, error bars = SEM, n=20.

(C) *nsy-1(ok593)* mutant animals have slow locomotion. ***, p<0.001, error bars = SEM, n=20.

(D) *nsy-1(ok593)* suppresses *egl-30(gf)*. *egl-30(gf) nsy-1* animals move more slowly than the hyperactive *egl-30(gf)* animals. ***, p< 0.001, error bars = SEM, n=20.

(E) *pmk-2, pmk-2 pmk-1,* and *pmk-3* mutant animals have slow locomotion. ***, p< 0.001; *, p<0.05, compared to WT, error bars = SEM, n=20.

(F) A *pmk-2 pmk-1* double mutant suppresses the hyperactivity of *egl-30(gf)*. ***, p< 0.001, error bars = SEM, n=20.

(G) A *pmk-2 pmk-1* double mutant suppresses the deep body bends of *egl-30(gf)*. *egl-30(gf)* animals with mutations in either *pmk-1, pmk-2,* or *pmk-3* are still small and loopy. *egl-30(gf) pmk-2 pmk-1* animals are less loopy and have a more wild-type posture.

Figure 4: *sek-1* acts in the same genetic pathway as *unc-73*

(A) *sek-1* does not act in the same genetic pathway as *egl-8.* The *sek-1(km4)* mutation enhances the slow locomotion of *egl-8(sa47)* mutants. ***, p< 0.001, error bars = SEM, n=20.

(B) *sek-1* does not act in the same genetic pathway as *rund-1*. The *sek-1(km4)* mutation enhances the slow locomotion of *rund-1(tm3622)* mutants. ***, p< 0.001, error bars = SEM, n=20.

bioRxiv preprint doi: https://doi.org/10.1101/093252; this version posted December 13, 2016. The copyright holder for this preprint (which was not certified by peer review) is the author/funder, who has granted bioRxiv a license to display the preprint in perpetuity. It is made available under aCC-BY-NC 4.0 International license.

(C) *sek-1* may act in the same genetic pathway as *unc-73*. The *sek-1(km4)* mutation does not enhance the slow locomotion phenotype of *unc-73* mutants. ns, p>0.05, error bars = SEM, n=20.

(D) *sek-1(km4)* does not suppress the high-amplitude waveform of *nzIs29 rho-1(gf)* animals. *rho-1(gf)* and *rho-1(gf) sek-1(km4)* animals have similar body posture.

(E) *sek-1(km4)* does not suppress the slow locomotion of *rho-1(gf)* animals. ***, p< 0.001, error bars = SEM, n=20.

Figure 5: *sek-1* and *nsy-1* weakly suppress *nca-1(gf)*

(a) *nca-1(gf)* mutants are small and tightly coiled. The phenotypes of these *nca-1(ox352)* animals are partially suppressed by *nsy-1(ok593)* and *sek-1(km4)*. Photos of first-day adults.

(b) *nsy-1* and *sek-1* suppress *nca-1(gf)* locomotion. *nca-1(gf)* animals travel a small distance from the center of the plate in the radial locomotion assay. *nca-1(gf) nsy-1(ok593)* and *nca-1(gf) sek-1(km4)* worms move further than *nca-1(gf)* worms. **, p<0.01; *, p<0.05. Error bars = SEM, n=30.

(c) Expression of *sek-1* in all neurons and in acetylcholine neurons partially reverts the *sek-1* mutant suppression of *nca-1(gf)* size and body posture. White arrowheads depict food piles created by *nca-1(gf) sek-1(km4)* animals due to their uncoordinated locomotion. Such food piles are not made by *nca-1(gf)* animals.

(d) None of the neuronal *sek-1* rescuing constructs revert the radial locomotion phenotype of *nca-1(gf) sek-1(km4)* animals. Although the pan-neuronal and acetylcholine neuron constructs revert the size phenotype of *nca-1(gf) sek-1(km4)*,

bioRxiv preprint doi: https://doi.org/10.1101/093252; this version posted December 13, 2016. The copyright holder for this preprint (which was not certified by peer review) is the author/funder, who has granted bioRxiv a license to display the preprint in perpetuity. It is made available under aCC-BY-NC 4.0 International license.

these animals do not move a significantly different distance than *nca-1(gf) sek-1(km4)* animals. ns, p>0.05. Error bars = SEM, n=19-24.

Figure S1: *sek-1* suppresses *egl-30(gf)* deep body bends

(a) *egl-30(gf)* mutants have deeper body bends than wild-type (WT) and *sek-1* mutations suppresses this loopy posture. Images show tracks of forward-moving first-day adults.

(b) Quantification of the waveform phenotype. ***, p<0.001, error bars = SEM, n=4-5.

(c) *sek-1(ag1)* mutant animals have slow locomotion. ***, p<0.001, error bars = SEM, n=10.

(d) *sek-1* suppresses *goa-1* hyperactivity. *goa-1(sa734) sek-1(km4)* animals move more slowly than *goa-1(sa734)* animals. ***, p<0.001, error bars = SEM, n=20.

Figure S2: Locomotion of p38 and JNK MAPK pathway mutants

(A) *tir-1(tm3036)* suppresses *egl-30(gf)*. *egl-30(gf) tir-1(tm3036)* animals are less loopy and have a more wild-type posture.

(B) *nsy-1(ok593)* suppresses *egl-30(gf)*. *egl-30(gf) nsy-1(ok593)* animals are less loopy and have a more wild-type posture.

(C) *jkk-1* and *jnk-1* act in parallel to *sek-1* and *pmk-2 pmk-1*. The *jnk-1(gk7) sek-1(km4)* double mutant and *pmk-2(qd279 qd171) pmk-1(km25) jkk-1(km2)* triple mutants move more slowly than the respective individual mutants. **, p< 0.01, *, p<0.05; error bars = SEM, n=20.

bioRxiv preprint doi: https://doi.org/10.1101/093252; this version posted December 13, 2016. The copyright holder for this preprint (which was not certified by peer review) is the author/funder, who has granted bioRxiv a license to display the preprint in perpetuity. It is made available under aCC-BY-NC 4.0 International license.

(D) Worms with gain-of-function or loss-of-function alleles of *atf-7* are slower than wild-type worms. p< 0.001, error bars = SEM, n=20.

(E) Worms lacking *gap-2* and *vhp-1* move like wild-type worms. Neither *gap-2(tm478)* nor *vhp-1(sa366)* confers a slow locomotion phenotype. ns, p>0.05 compared to WT, error bars = SEM, n=20.

(F-G) *tir-1(ky648gf)* animals do not have loopy or hyperactive locomotion. *tir-1(ky648gf)* worms have wild-type posture and are slower than wild-type animals. ***, p< 0.001, error bars = SEM, n=20.

Table S1: Strain List

Strain	Genotype
AU1	*sek-1(ag1)* X
BS3383	*pmk-3(ok169)* IV
CX3695	*kyIs140[str-2p::gfp, lin-15(+)]* I
CX5959	*kyIs140[str-2p::gfp, lin-15(+)]* I; *tir-1(ky648gf)* III
EG317	*unc-73(ox317)* I
EG1000	*dpy-5(e61)* I; *rol-6(e187)* II; *lon-1(e1820)* III
EG1020	*bli-6(sc16)* IV; *dpy-11(e224)* V; *lon-2(e678)* X
EG4782	*nzIs29[unc-17p::rho-1(G14V), unc-122::gfp]* II
EG5505	*rund-1(tm3622)* X
EG7989	*unc-119(ed3)* III; *oxTi668[eft-3p::TdTomato::H2B, Cb-unc-119(+)]* X
IG685	*tir-1(tm3036)* III
JN147	*gap-2(tm748)* X

bioRxiv preprint doi: https://doi.org/10.1101/093252; this version posted December 13, 2016. The copyright holder for this preprint (which was not certified by peer review) is the author/funder, who has granted bioRxiv a license to display the preprint in perpetuity. It is made available under aCC-BY-NC 4.0 International license.

JT47	*egl-8(sa47)* V
JT366	*vhp-1(sa366)* II
JT734	*goa-1(sa734)* I
KU2	*jkk-1(km2)* X
KU4	*sek-1(km4)* X
KU25	*pmk-1(km25)* IV
N2	Bristol wild isolate, standard lab wild-type
VC8	*jnk-1(gk7)* IV
VC390	*nsy-1(ok593)* IV
XZ42	*sek-1(yak42)* X
XZ1233	*egl-30(tg26)* I*; sek-1(yak42)* X
XZ1151	*egl-30(tg26)* I
XZ1566	*egl-8(sa47)* V*; sek-1(yak42)* X
XZ1567	*unc-73(ox317)* I*; sek-1(yak42)* X
XZ1574	*rund-1(tm3622) sek-1(yak42)* X
XZ1575	*egl-30(tg26)* I*; sek-1(km4)* X
XZ1588	*egl-30(tg26)* I*; nsy-1(ok593)* IV
XZ1589	*egl-30(tg26)* I*; sek-1(km4)* X*; qdEx8[unc-119p::sek-1::GFP, myo-2p::mStrawberry::unc-54-3'UTR]*
XZ1593	*egl-30(tg26)* I*; pmk-1(km25)* IV
XZ1642	*sek-1(km4)* X*; yakEx72[unc-17p::sek-1::tbb-2utr-operon-GFP::H2B::cye-1utr, myo-2p::mCherry]*
XZ1643	*sek-1(km4) X; yakEx73[unc-47p::sek-1::tbb-2utr-operon-GFP::H2B::cye-*

bioRxiv preprint doi: https://doi.org/10.1101/093252; this version posted December 13, 2016. The copyright holder for this preprint (which was not certified by peer review) is the author/funder, who has granted bioRxiv a license to display the preprint in perpetuity. It is made available under aCC-BY-NC 4.0 International license.

	1utr, myo-2p::mCherry]
XZ1717	*nzIs29[unc-17p::rho-1(G14V) unc-122::gfp]* II*; sek-1(km4)* X
XZ1770	*egl-30(tg26)* I*; pmk-2(qd279 qd171) pmk-1(km25)* IV
XZ1771	*egl-30(tg26)* I*; pmk-2(qd287)* IV
XZ1772	*egl-30(tg26)* I*; pmk-3(ok169)* IV
XZ1815	*egl-30(tg26)* I*; tir-1(tm3036)* III
XZ1816	*nca-1(ox352)* IV*; sek-1(km4)* X*; qdEx8[unc-119p::sek-1::GFP::unc-54-3' UTR, myo-2p::mStrawberry::unc-54-3'UTR]*
XZ1834	*egl-30(tg26)* I*; sek-1(km4)* X*; yakEx72[unc-17p::sek-1::tbb-2utr-operon-GFP::H2B::cye-1utr, myo-2p::mCherry]*
XZ1835	*nca-1(ox352)* IV*; sek-1(km4)* X*; yakEx72[unc-17p::sek-1::tbb-2utr-operon-GFP::H2B::cye-1utr, myo-2p::mCherry]*
XZ1861	*nca-1(ox352)* IV*; sek-1(km4)* X*; yakEx73[unc-47p::sek-1::tbb-2utr-operon-GFP::H2B::cye-1utr, myo-2p::mCherry]*
XZ1863	*egl-30(tg26)* I*; sek-1(km4)* X*; yakEx73[unc-47p::sek-1::tbb-2utr-operon-GFP::H2B::cye-1utr, myo-2p::mCherry]*
XZ1872	*jnk-1(gk7)* I*; sek-1(km4)* X
XZ1873	*pmk-2(qd279 qd171) pmk-1(km25)* IV*; jkk-1(km2)* X
XZ1937	*sek-1(km4)* X*; yakEx121[hsp-16.2p::sek-1::tbb-2-3' UTR::gld-1 operon linker::gfp::h2b, myo-2p::mCherry]*
XZ1939	*goa-1(sa734)* I*; sek-1(km4)* X
XZ1942	*tir-1(ky648gf)* III
ZD202	*sek-1(km4)* X*; qdEx8[unc-119p::sek-1::GFP::unc-54-3' UTR + myo-*

bioRxiv preprint doi: https://doi.org/10.1101/093252; this version posted December 13, 2016. The copyright holder for this preprint (which was not certified by peer review) is the author/funder, who has granted bioRxiv a license to display the preprint in perpetuity. It is made available under aCC-BY-NC 4.0 International license.

	2p::mStrawberry::unc-54-3'UTR]
ZD318	*agIs29 atf-7(qd22 qd130)* III
ZD442	*agIs29 atf-7(qd22)* III
ZD934	*pmk-2(qd279 qd171) pmk-1(km25)* IV
ZD1020	*pmk-2(qd287)* IV

Table S2: Plasmids and Primers

Gateway entry clones

Plasmid	Details
pJH21	*sek-1* cDNA [1-2]
pCFJ150	pDEST5605[4-3]
pCFJ326	*tbb-2utr-operon-GFP::H2B::cye-1utr* [2-3]
pMH522	*unc-47p* [4-1]
pGH1	*unc-17p* [4-1]
pCM1.56	*hsp-16.2p* [4-1]

Gateway Expression Constructs

Plasmid	Details	Used to make
pJH23	*unc-17p::sek-1:: tbb-2utr-operon-GFP::H2B::cye-1utr*	*yakEx72*
pJH24	*unc-47p::sek-1:: tbb-2utr-operon-GFP::H2B::cye-1utr*	*yakEx73*
pJH46	*hsp-16.2p::sek-1:: tbb-2utr-*	*yakEx121*

bioRxiv preprint doi: https://doi.org/10.1101/093252; this version posted December 13, 2016. The copyright holder for this preprint (which was not certified by peer review) is the author/funder, who has granted bioRxiv a license to display the preprint in perpetuity. It is made available under aCC-BY-NC 4.0 International license.

	operon-GFP::H2B::cye-1utr	

Primers

oJH114	GGGGACAAGTTTGTACAAAAAAGCAGGCTcaATGGAGCGAAAAGGACGTG	F to clone *sek-1* cDNA into [1-2]
oJH115	GGGGACCACTTTGTACAAGAAAGCTGGGTgTCATCGTCGCCAAACAGTG	R to clone *sek-1* cDNA into [1-2]

Table S3: Statistical Tests

Figure	Test	p value
1C	One-way ANOVA and Bonferroni's Multiple Comparison Test WT vs *egl-30(tg26)* (p<0.001) *egl-30(tg26)* vs *egl-30(tg26); sek-1(yak42)* (p<0.001) *egl-30(tg26)* vs *egl-30(tg26);sek-1(km4)* (p<0.001)	< 0.001
1D	One-way ANOVA and Dunnett's Multiple Comparison Test WT vs *sek-1(yak42)* (p<0.001) WT vs *sek-1(km4)* (p<0.001)	< 0.001

bioRxiv preprint doi: https://doi.org/10.1101/093252; this version posted December 13, 2016. The copyright holder for this preprint (which was not certified by peer review) is the author/funder, who has granted bioRxiv a license to display the preprint in perpetuity. It is made available under aCC-BY-NC 4.0 International license.

2A	One-way ANOVA and Bonferroni's Multiple Comparison Test *sek-1(km4)* vs *sek-1(km4); qdEx8[unc-119p::sek-1(+)]* (p<0.001)	< 0.001
2B	One-way ANOVA and Bonferroni's Multiple Comparison Test *sek-1(km4)* vs *sek-1(km4); yakEx72[unc-17p::sek-1(+)]* (p<0.001) *sek-1(km4)* vs *sek-1(km4); yakEx73[unc-47p::sek-1(+)]* (ns)	< 0.001
2D	Kruskal-Wallis Test and Dunn's Multiple Comparison Test *egl-30(tg26); sek-1(km4)* vs *egl-30(tg26); sek-1(km4); qdEx8[unc-119p::sek-1(+)]* (p<0.001) *egl-30(tg26); sek-1(km4)* vs *egl-30(tg26); sek-1(km4); yakEx72[unc-17p::sek-1(+)]* (p<0.01) *egl-30(tg26); sek-1(km4)* vs *egl-30(tg26); sek-1(km4); yakEx73[unc-47p::sek-1(+)]* (ns)	< 0.001
2E	One-way ANOVA and Bonferroni's Multiple Comparison Test *sek-1(km4)* vs *sek-1(km4); yakEx121[hsp-16.2p::sek-1(+)]* (p<0.001)	< 0.001
3A	Unpaired t test, two-tailed	< 0.001

bioRxiv preprint doi: https://doi.org/10.1101/093252; this version posted December 13, 2016. The copyright holder for this preprint (which was not certified by peer review) is the author/funder, who has granted bioRxiv a license to display the preprint in perpetuity. It is made available under aCC-BY-NC 4.0 International license.

3B	One-way ANOVA and Bonferroni's Multiple Comparison Test *egl-30(tg26)* vs *egl-30(tg26); tir-1(tm3036)* (p<0.001)	< 0.001
3C	Unpaired t test, two-tailed	< 0.001
3D	One-way ANOVA and Bonferroni's Multiple Comparison Test *egl-30(tg26)* vs *egl-30(tg26); nsy-1(ok593)* (p<0.001)	< 0.001
3E	One-way ANOVA and Dunnett's Multiple Comparison Test WT vs *pmk-1(km25)* (ns) WT vs *pmk-2(qd287)* (p<0.05) WT vs *pmk-2(qd279 qd171) pmk-1 (km25)* (p<0.001) WT vs *pmk-3(ok169)* (p<0.001)	< 0.001
3F	One-way ANOVA and Dunnett's Multiple Comparison Test *egl-30(tg26)* vs *egl-30(tg26); pmk-1(km25)* (p<0.001) *egl-30(tg26)* vs *egl-30(tg26); pmk-2(qd287)* (p<0.001) *egl-30(tg26)* vs *egl-30(tg26); pmk-2(qd279 qd171) pmk-1 (km25)* (p<0.001) *egl-30(tg26)* vs *egl-30(tg26); pmk-3(ok169)* (p<0.001)	< 0.001
4A	One-way ANOVA and Bonferroni's Multiple Comparison Test *egl-8(sa47)* vs *egl-8(sa47); sek-1(yak42)* (p<0.001)	< 0.001
4B	One-way ANOVA and Bonferroni's Multiple Comparison Test	< 0.001

bioRxiv preprint doi: https://doi.org/10.1101/093252; this version posted December 13, 2016. The copyright holder for this preprint (which was not certified by peer review) is the author/funder, who has granted bioRxiv a license to display the preprint in perpetuity. It is made available under aCC-BY-NC 4.0 International license.

	sek-1(yak42) vs *rund-1(tm3622); sek-1(yak42)* (p<0.001)	
4C	One-way ANOVA and Bonferroni's Multiple Comparison Test *unc-73(ox317)* vs *unc-73(ox317); sek-1(yak42)* (ns)	< 0.001
4E	One-way ANOVA and Bonferroni's Multiple Comparison Test *nzIs29[unc-17p::rho-1(G14V)]* vs *nzIs29[unc-17p::rho-1(G14V)]; sek-1(km4)* (p<0.001)	< 0.001
5B	One-way ANOVA and Bonferroni's Multiple Comparison Test WT vs *nca-1(ox352)* (p<0.001) *nca-1(ox352)* vs *nca-1(ox352); nsy-1(ok593)* (p<0.01) *nca-1(ox352)* vs *nca-1(ox352); sek-1(km4)* (p<0.05)	< 0.001
5D	Kruskal-Wallis Test and Dunn's Multiple Comparison Test *nca-1(ox352);sek-1(km4)* vs *nca-1(ox352);sek-1(km4); qdEx8[unc-119p::sek-1(+)]* (ns) *nca-1(ox352);sek-1(km4)* vs *nca-1(ox352);sek-1(km4); yakEx72[unc-17p::sek-1(+)]* (ns) *nca-1(ox352);sek-1(km4)* vs *nca-1(ox352);sek-1(km4); yakEx73[unc-47p::sek-1(+)]* (ns)	< 0.001
S1B	One-way ANOVA and Bonferroni's Multiple Comparison Test *egl-30(tg26)* vs *egl-30(tg26); sek-1(yak42)*	< 0.001

bioRxiv preprint doi: https://doi.org/10.1101/093252; this version posted December 13, 2016. The copyright holder for this preprint (which was not certified by peer review) is the author/funder, who has granted bioRxiv a license to display the preprint in perpetuity. It is made available under aCC-BY-NC 4.0 International license.

	(p<0.001) *egl-30(tg26)* vs *egl-30(tg26); sek-1(km4)* (p<0.001)	
S1C	One-way ANOVA and Newman-Keuls Multiple Comparison Test WT vs *sek-1(yak42)* (p<0.001) WT vs *sek-1(ag1)* (p<0.001) *sek-1(yak42)* vs *sek-1(ag1)* (ns)	< 0.001
S1D	One-way ANOVA and Bonferroni's Multiple Comparison Test WT vs *sek-1(km4)* (p<0.001) *goa-1(sa734)* vs *sek-1(km4)* (p<0.001) *goa-1(sa734); sek-1(km4)* vs *sek-1(km4)* (p<0.001)	< 0.001
S2C	One-way ANOVA and Bonferroni's Multiple Comparison Test *jnk-1(gk7)* vs *jnk-1(gk7); sek-1(km4)* (p<0.01) *jkk-1(km2) vs pmk-2(qd279 qd171) pmk-1 (km25); jkk-1(km2)* (p<0.05)	< 0.001
S2D	One-way ANOVA and Bonferroni's Multiple Comparison Test WT vs *atf-7(qd22)* (p<0.001) WT vs *atf-7(qd22 qd130)* (p<0.001)	< 0.001
S2E	One-way ANOVA	p=0.806

bioRxiv preprint doi: https://doi.org/10.1101/093252; this version posted December 13, 2016. The copyright holder for this preprint (which was not certified by peer review) is the author/funder, who has granted bioRxiv a license to display the preprint in perpetuity. It is made available under aCC-BY-NC 4.0 International license.

S2G	Unpaired t test, two-tailed	< 0.001

References

Ailion, M., M. Hannemann, S. Dalton, A. Pappas, S. Watanabe, *et al.,* 2014 Two Rab2 interactors regulate dense-core vesicle maturation. Neuron 82: 167–180.

Andrusiak, M. G., and Y. Jin, 2016 Context Specificity of Stress-activated Mitogen-activated Protein (MAP) Kinase Signaling: The Story as Told by *Caenorhabditis elegans*. J. Biol. Chem. 291: 7796–7804.

Bastiani, C. A., S. Gharib, M. I. Simon, and P. W. Sternberg, 2003 Caenorhabditis elegans Gαq Regulates Egg-Laying Behavior via a PLCβ-Independent and Serotonin-Dependent Signaling Pathway and Likely Functions Both in the Nervous System and in Muscle. Genetics 165: 1805–1822.

Bence, K., W. Ma, T. Kozasa, and X. -Y. Huang, 1997 Direct stimulation of Bruton's tyrosine kinase by Gq-protein α-subunit. Nature 389: 296–299.

Bolshakov V. Y., Carboni L., Cobb M. H., Siegelbaum S. A., Belardetti F., 2000 Dual MAP kinase pathways mediate opposing forms of long-term plasticity at CA3-CA1 synapses. Nat. Neurosci. **3**: 1107–1112.

Brenner, S., 1974 The genetics of Caenorhabditis elegans. Genetics 77: 71–94.

Chang, C., Y. -W. Hsieh, B. J. Lesch, C. I. Bargmann, and C. -F. Chuang, 2011 Microtubule-based localization of a synaptic calcium-signaling complex is required for left-right neuronal asymmetry in *C. elegans*. Development 138: 3509–3518.

bioRxiv preprint doi: https://doi.org/10.1101/093252; this version posted December 13, 2016. The copyright holder for this preprint (which was not certified by peer review) is the author/funder, who has granted bioRxiv a license to display the preprint in perpetuity. It is made available under aCC-BY-NC 4.0 International license.

Chuang, C. -F., and C. I. Bargmann, 2005 A Toll-interleukin 1 repeat protein at the synapse specifies asymmetric odorant receptor expression via ASK1 MAPKKK signaling. Genes Dev. 19: 270–281.

Couillault, C., N. Pujol, J. Reboul, L. Sabatier, J. -F. Guichou, *et al*., 2004 TLR-independent control of innate immunity in Caenorhabditis elegans by the TIR domain adaptor protein TIR-1, an ortholog of human SARM. Nat. Immunol. 5: 488–494.

Doi, M., and K. Iwasaki, 2002 Regulation of Retrograde Signaling at Neuromuscular Junctions by the Novel C2 Domain Protein AEX-1. Neuron 33: 249–259.

Fay, D. 2006 Genetic mapping and manipulation: Chapter 7-Making compound mutants. *WormBook*, ed. The *C. elegans* Research Community, WormBook, doi/10.1895/wormbook.1.96.2, http://www.wormbook.org

Frøkjær-Jensen, C., M. W. Davis, M. Ailion, and E. M. Jorgensen 2012 Improved Mos1-mediated transgenesis in *C. elegans*. Nat. Methods 9: 117–118.

Frokjaer-Jensen, C., M. W. Davis, M. Sarov, J. Taylor, S. Flibotte, *et al*., 2014 Random and targeted transgene insertion in C. elegans using a modified Mosl transposon. Nat. Methods 11: 529–534.

Gao, S., L. Xie, T. Kawano, M. D. Po, J. K. Pirri, *et al*., 2015 The NCA sodium leak channel is required for persistent motor circuit activity that sustains locomotion. Nat. Commun. 6: 6323.

bioRxiv preprint doi: https://doi.org/10.1101/093252; this version posted December 13, 2016. The copyright holder for this preprint (which was not certified by peer review) is the author/funder, who has granted bioRxiv a license to display the preprint in perpetuity. It is made available under aCC-BY-NC 4.0 International license.

García-Hoz, C., G. Sánchez-Fernández, M. T. Díaz-Mec, J. Moscat, F. Mayor *et al.*, 2010 Gαq Acts as an Adaptor Protein in Protein Kinase Cζ (PKCζ)-mediated ERK5 Activation by G Protein-coupled Receptors (GPCR). J. Biol. Chem. 285: 13480–13489.

Hajdu-Cronin, Y. M., W. J. Chen, G. Patikoglou, M. R. Koelle, and P. W. Sternberg, 1999 Antagonism between Goα and Gqα in Caenorhabditis elegans: the RGS protein EAT-16 is necessary for Goα signaling and regulates Gqα activity. Genes Dev. 13: 1780–1793.

Hoppe, P. E., J. Chau, K. A. Flanagan, A. R. Reedy, and L. A. Schriefer, 2010 *Caenorhabditis elegans unc-82* Encodes a Serine/Threonine Kinase Important for Myosin Filament Organization in Muscle During Growth. Genetics 184: 79–90.

Huang, C. -C., J. -L. You, M. -Y. Wu, and K. -S. Hsu, 2004 Rap1-induced p38 mitogen-activated protein kinase activation facilitates AMPA receptor trafficking via the GDI.Rab5 complex. Potential role in (S)-3,5-dihydroxyphenylglycene-induced long term depression. J. Biol. Chem. 279: 12286–12292.

Hudmon, A., J. -S. Choi, L. Tyrrell, J. A. Black, A. M. Rush, *et al*., 2008 Phosphorylation of Sodium Channel Nav1.8 by p38 Mitogen-Activated Protein Kinase Increases Current Density in Dorsal Root Ganglion Neurons. J. Neurosci. 28: 3190–3201.

Inoue, H., N. Hisamoto, J. H. An, R. P. Oliveira, E. Nishida, *et al*., 2005 The *C. elegans* p38 MAPK pathway regulates nuclear localization of the transcription factor SKN-1 in oxidative stress response. Genes Dev. 19: 2278–2283.

bioRxiv preprint doi: https://doi.org/10.1101/093252; this version posted December 13, 2016. The copyright holder for this preprint (which was not certified by peer review) is the author/funder, who has granted bioRxiv a license to display the preprint in perpetuity. It is made available under aCC-BY-NC 4.0 International license.

Jantsch-Plunger, V., P. Gönczy, A. Romano, H. Schnabel, D. Hamill, *et al.*, 2000 CYK-4: A Rho family gtpase activating protein (GAP) required for central spindle formation and cytokinesis. J. Cell Biol. 149: 1391–1404.

Kawasaki, M., N. Hisamoto, Y. Iino, M. Yamamoto, J. Ninomiya-Tsuji , *et al.*, 1999 A *Caenorhabditis elegans* JNK signal transduction pathway regulates coordinated movement via type-D GABAergic motor neurons. EMBO J. 18: 3604–3615.

Kim, D.H., R. Feinbaum, G. Alloing, F. E. Emerson, D. A. Garsin, *et al.*, 2002 A Conserved p38 MAP Kinase Pathway in *Caenorhabditis elegans* Innate Immunity. Science 297: 623–626.

Kim, D.H., N. T. Liberati, T. Mizuno, H. Inoue, N. Hisamoto, *et al.*, 2004 Integration of *Caenorhabditis elegans* MAPK pathways mediating immunity and stress resistance by MEK-1 MAPK kinase and VHP-1 MAPK phosphatase. Proc. Natl. Acad. Sci. U. S. A. 101: 10990–10994.

Koelle, M. R., 2016 Neurotransmitter signaling through heterotrimeric G proteins: insights from studies in *C. elegans*. WormBook, doi:10.1895/wormbook.1.75.2.

Kyriakis, J. M., and J. Avruch, 2012 Mammalian MAPK signal transduction pathways activated by stress and inflammation: a 10-year update. Physiol. Rev. 92:689-737.

Lackner, M. R., S. J. Nurrish, and J. M. Kaplan, 1999 Facilitation of Synaptic Transmission by EGL-30 Gqα and EGL-8 PLCβ: DAG Binding to UNC-13 Is Required to Stimulate Acetylcholine Release. Neuron 24: 335–346.

bioRxiv preprint doi: https://doi.org/10.1101/093252; this version posted December 13, 2016. The copyright holder for this preprint (which was not certified by peer review) is the author/funder, who has granted bioRxiv a license to display the preprint in perpetuity. It is made available under aCC-BY-NC 4.0 International license.

Lu, B., Y. Su, S. Das, J. Liu, J. Xia, *et al*., 2007 The Neuronal Channel NALCN Contributes Resting Sodium Permeability and Is Required for Normal Respiratory Rhythm. Cell 129: 371–383.

McMullan, R., E. Hiley, P. Morrison, and S. J. Nurrish 2006 Rho is a presynaptic activator of neurotransmitter release at pre-existing synapses in *C. elegans*. Genes Dev. 20: 65–76.

Mello, C. C., J. M. Kramer, D. Stinchcomb, and V. Ambros, 1991 Efficient gene transfer in C.elegans: extrachromosomal maintenance and integration of transforming sequences. EMBO J. 10: 3959–3970.

Miller, K. G., M. D. Emerson, and J. B. Rand 1999 Goα and Diacylglycerol Kinase Negatively Regulate the Gqα Pathway in *C. elegans*. Neuron 24: 323–333.

Minevich, G., D. S. Park, D. Blankenberg, R. J. Poole, and O. Hobert, 2012 CloudMap: a cloud-based pipeline for analysis of mutant genome sequences. Genetics 192: 1249–1269.

Nash, H. A., R. L. Scott, B. C. Lear, and R. Allada, 2002 An unusual cation channel mediates photic control of locomotion in *Drosophila*. Curr. Biol. 12: 2152–2158.

Nurrish S., Ségalat L., Kaplan J. M., 1999 Serotonin inhibition of synaptic transmission: Galpha(0) decreases the abundance of UNC-13 at release sites. Neuron 24: 231–242.

bioRxiv preprint doi: https://doi.org/10.1101/093252; this version posted December 13, 2016. The copyright holder for this preprint (which was not certified by peer review) is the author/funder, who has granted bioRxiv a license to display the preprint in perpetuity. It is made available under aCC-BY-NC 4.0 International license.

Pagano, D. J., E. R. Kingston, and D. H. Kim, 2015 Tissue Expression Pattern of PMK-2 p38 MAPK Is Established by the miR-58 Family in *C. elegans*. PLOS Genet 11: e1004997.

Park, E.C., and Rongo, C. (2016). The p38 MAP kinase pathway modulates the hypoxia response and glutamate receptor trafficking in aging neurons. eLife *5*, e12010.

Plowman, G. D., S. Sudarsanam, J. Bingham, D. Whyte, and T. Hunter, 1999 The protein kinases of *Caenorhabditis elegans*: a model for signal transduction in multicellular organisms. Proc. Natl. Acad. Sci. U. S. A. 96: 13603–13610.

Rhee, S. G. 2001 Regulation of Phosphoinositide-Specific Phospholipase C. Annu. Rev. Biochem. 70: 281–312.

Rush A. M., Wu J., Rowan M. J., Anwyl R., 2002 Group I metabotropic glutamate receptor (mGluR)-dependent long-term depression mediated via p38 mitogen-activated protein kinase is inhibited by previous high-frequency stimulation and activation of mGluRs and protein kinase C in the rat dentate gyrus in vitro. J. Neurosci. 22: 6121–6128.

Sagasti, A., N. Hisamoto, J. Hyodo, M. Tanaka-Hino, K. Matsumoto, *et al.*, (2001). The CaMKII UNC-43 Activates the MAPKKK NSY-1 to Execute a Lateral Signaling Decision Required for Asymmetric Olfactory Neuron Fates. Cell 105: 221–232.

Sánchez-Fernández, G., S. Cabezudo, C. García-Hoz, C. Benincá, A. M. Aragay, *et al.*, (2014). Gαq signalling: The new and the old. Cell. Signal. 26: 833–848.

bioRxiv preprint doi: https://doi.org/10.1101/093252; this version posted December 13, 2016. The copyright holder for this preprint (which was not certified by peer review) is the author/funder, who has granted bioRxiv a license to display the preprint in perpetuity. It is made available under aCC-BY-NC 4.0 International license.

Shi, Y., C. Abe, B. B. Holloway, S. Shu, N. N. Kumar, *et al.*, 2016 Nalcn Is a "Leak" Sodium Channel That Regulates Excitability of Brainstem Chemosensory Neurons and Breathing. J. Neurosci. 36: 8174–8187.

Shivers, R. P., D. J. Pagano, T. Kooistra, C. E. Richardson, K. C. Reddy, *et al*., 2010 Phosphorylation of the conserved transcription factor ATF-7 by PMK-1 p38 MAPK regulates innate immunity in *Caenorhabditis elegans*. PLoS Genet. 6: e1000892.

Tanaka-Hino, M., A. Sagasti, N. Hisamoto, M. Kawasaki, S. Nakano, *et al*., 2002 SEK-1 MAPKK mediates Ca2+ signaling to determine neuronal asymmetric development in *Caenorhabditis elegans*. EMBO Rep. 3: 56–62.

Topalidou, I., J. Cattin-Ortolá, A. L. Pappas, K. Cooper, G. E. Merrihew, *et al*., 2016a The EARP Complex and Its Interactor EIPR-1 Are Required for Cargo Sorting to Dense-Core Vesicles. PLOS Genet 12: e1006074.

Topalidou I., Chen P.-A., Cooper K., Watanabe S., Jorgensen E. M., *et al*.., 2016b The NCA-1 ion channel functions downstream of Gq and Rho to regulate locomotion in C. elegans. bioRxiv. doi: http://dx.doi.org/10.1101/090514

Vaqué, J. P., R. T. Dorsam, X. Feng, R. Iglesias-Bartolome, D. J. Forsthoefel, *et al.*, 2013 A genome-wide RNAi screen reveals a Trio-regulated Rho GTPase circuitry transducing mitogenic signals initiated by G protein-coupled receptors. Mol. Cell 49: 94–108.

Vashlishan, A. B., J. M. Madison, M. Dybbs, M., J. Bai, D. Sieburth, *et al.*, 2008 An RNAi Screen Identifies Genes that Regulate GABA Synapses. Neuron 58: 346–361.

bioRxiv preprint doi: https://doi.org/10.1101/093252; this version posted December 13, 2016. The copyright holder for this preprint (which was not certified by peer review) is the author/funder, who has granted bioRxiv a license to display the preprint in perpetuity. It is made available under aCC-BY-NC 4.0 International license.

Williams, S. L., S. Lutz, N. K. Charlie, C. Vettel, M. Ailion, *et al.*, 2007 Trio's Rho-specific GEF domain is the missing Galpha q effector in *C. elegans*. Genes Dev. 21: 2731–2746.

Wittmack, E. K., A. M. Rush, A. Hudmon, S. G. Waxman, and S. D. Dib-Hajj, 2005 Voltage-Gated Sodium Channel Nav1.6 Is Modulated by p38 Mitogen-Activated Protein Kinase. J. Neurosci. 25: 6621–6630.

Xie, Y., M. Moussaif, S. Choi, L. Xu, and J. Y. Sze, 2013 RFX transcription factor DAF-19 regulates 5-HT and innate immune responses to pathogenic bacteria in *Caenorhabditis elegans*. PLoS Genet. 9: e1003324.

Zhang, R., X. He, W. Liu, M. Lu, J. -T. Hsieh, *et al.*, 2003 AIP1 mediates TNF-α–induced ASK1 activation by facilitating dissociation of ASK1 from its inhibitor 14-3-3. J. Clin. Invest. 111: 1933–1943.

Figure 1

bioRxiv preprint doi: https://doi.org/10.1101/093252; this version posted December 13, 2016. The copyright holder for this preprint (which was not certified by peer review) is the author/funder, who has granted bioRxiv a license to display the preprint in perpetuity. It is made available under aCC-BY-NC 4.0 International license.

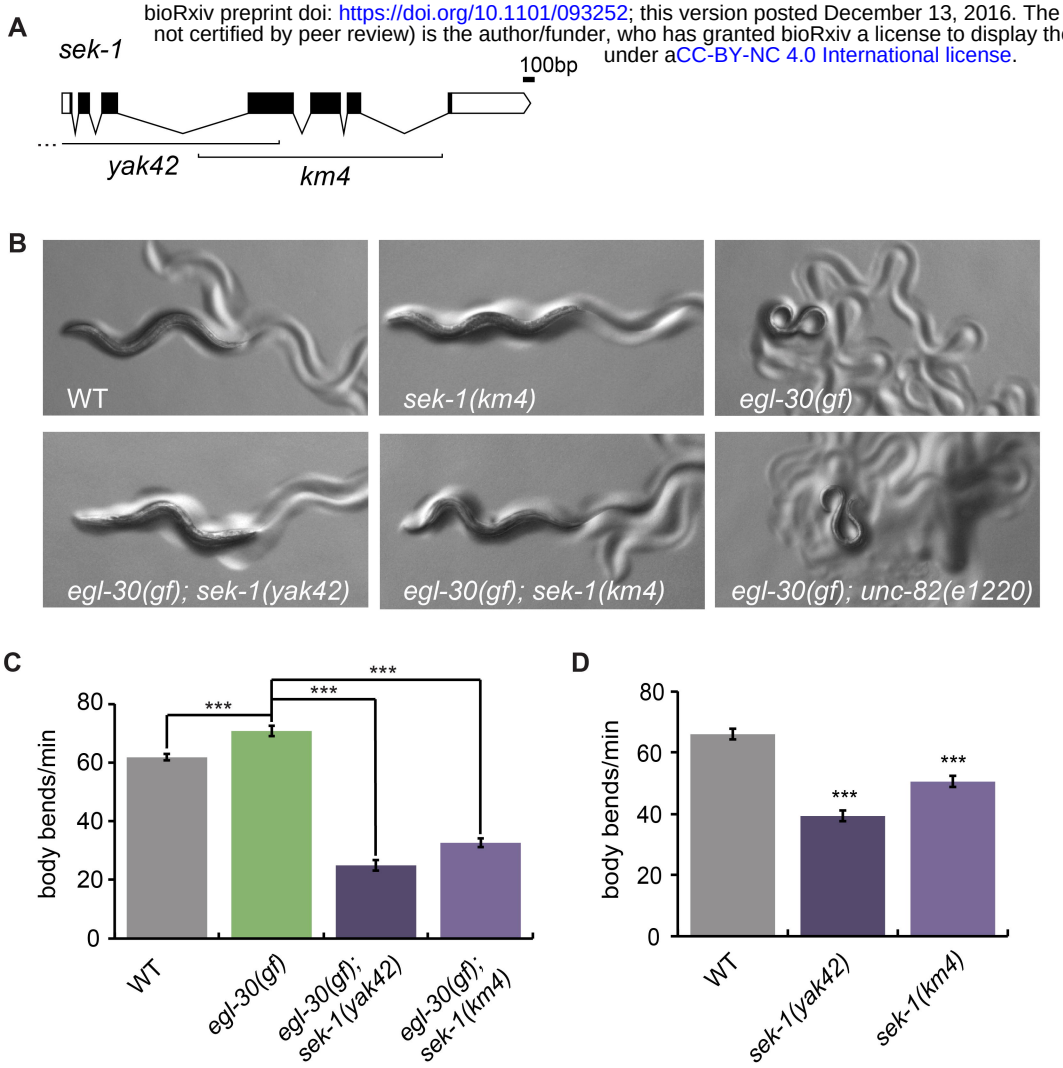

bioRxiv preprint doi: https://doi.org/10.1101/093252; this version posted December 13, 2016. The copyright holder for this preprint (which was not certified by peer review) is the author/funder, who has granted bioRxiv a license to display the preprint in perpetuity. It is made available under aCC-BY-NC 4.0 International license.

Figure 2

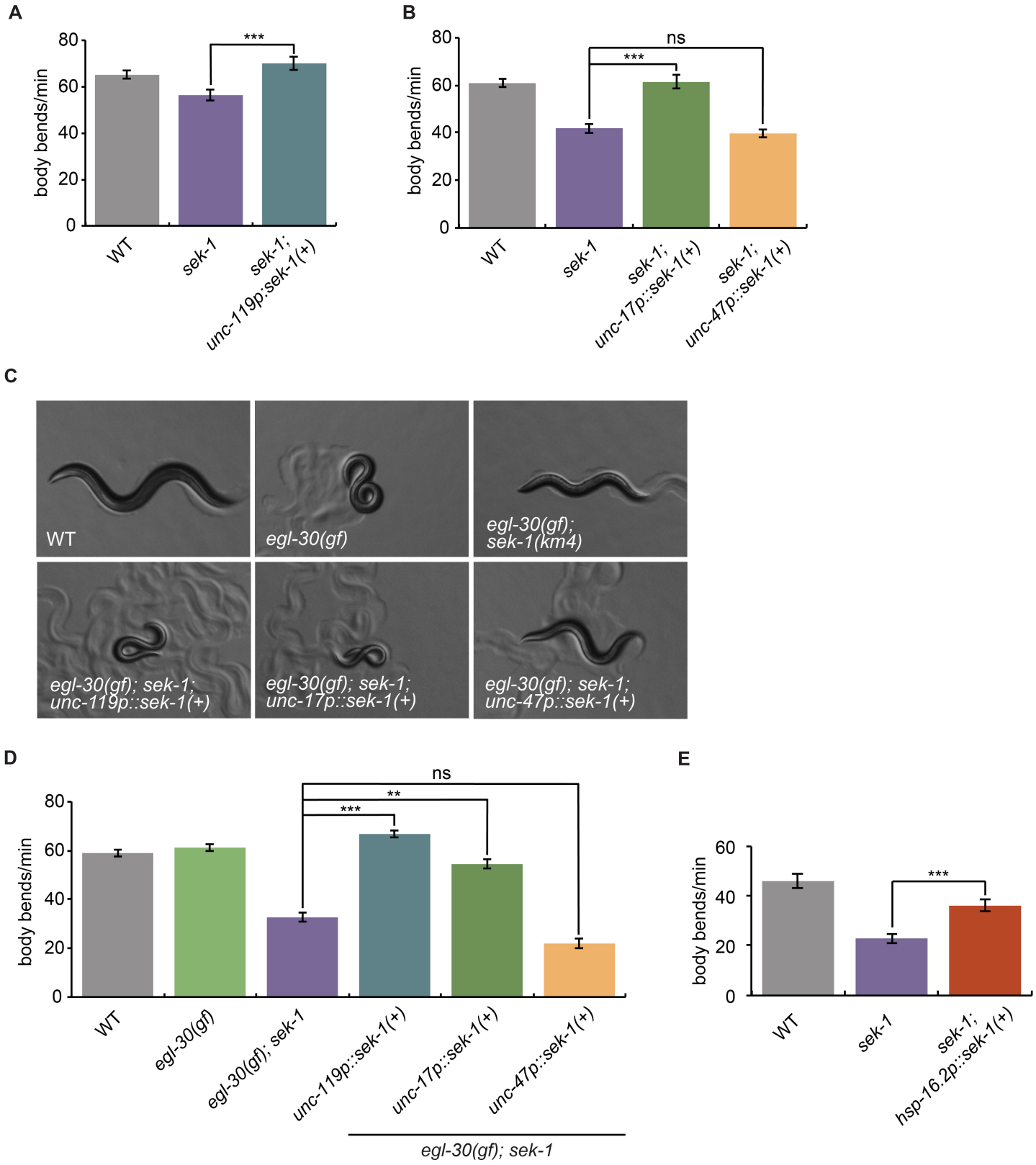

bioRxiv preprint doi: https://doi.org/10.1101/093252; this version posted December 13, 2016. The copyright holder for this preprint (which was not certified by peer review) is the author/funder, who has granted bioRxiv a license to display the preprint in perpetuity. It is made available under aCC-BY-NC 4.0 International license.

Figure 3

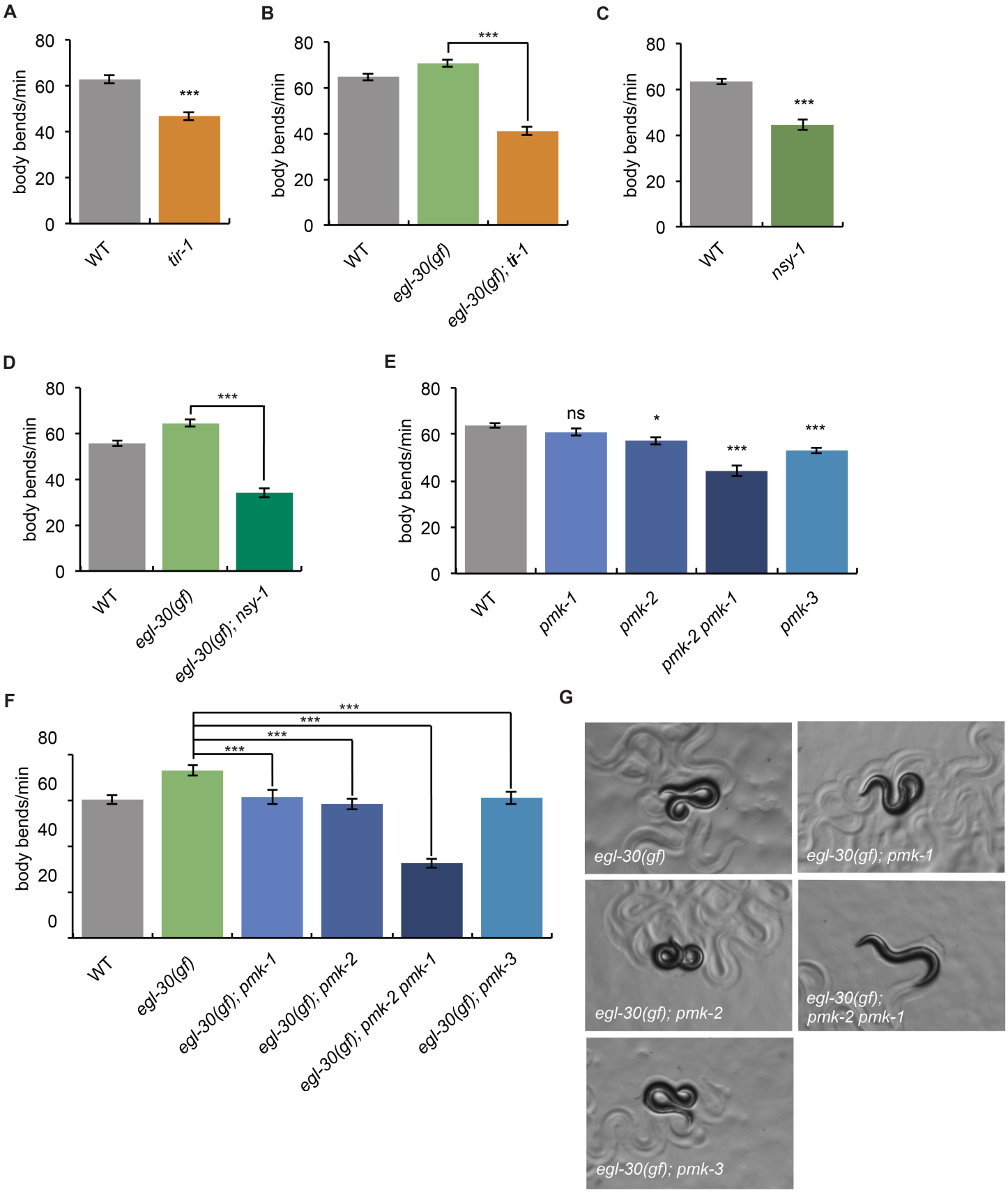

bioRxiv preprint doi: https://doi.org/10.1101/093252; this version posted December 13, 2016. The copyright holder for this preprint (which was not certified by peer review) is the author/funder, who has granted bioRxiv a license to display the preprint in perpetuity. It is made available under aCC-BY-NC 4.0 International license.

Figure 4

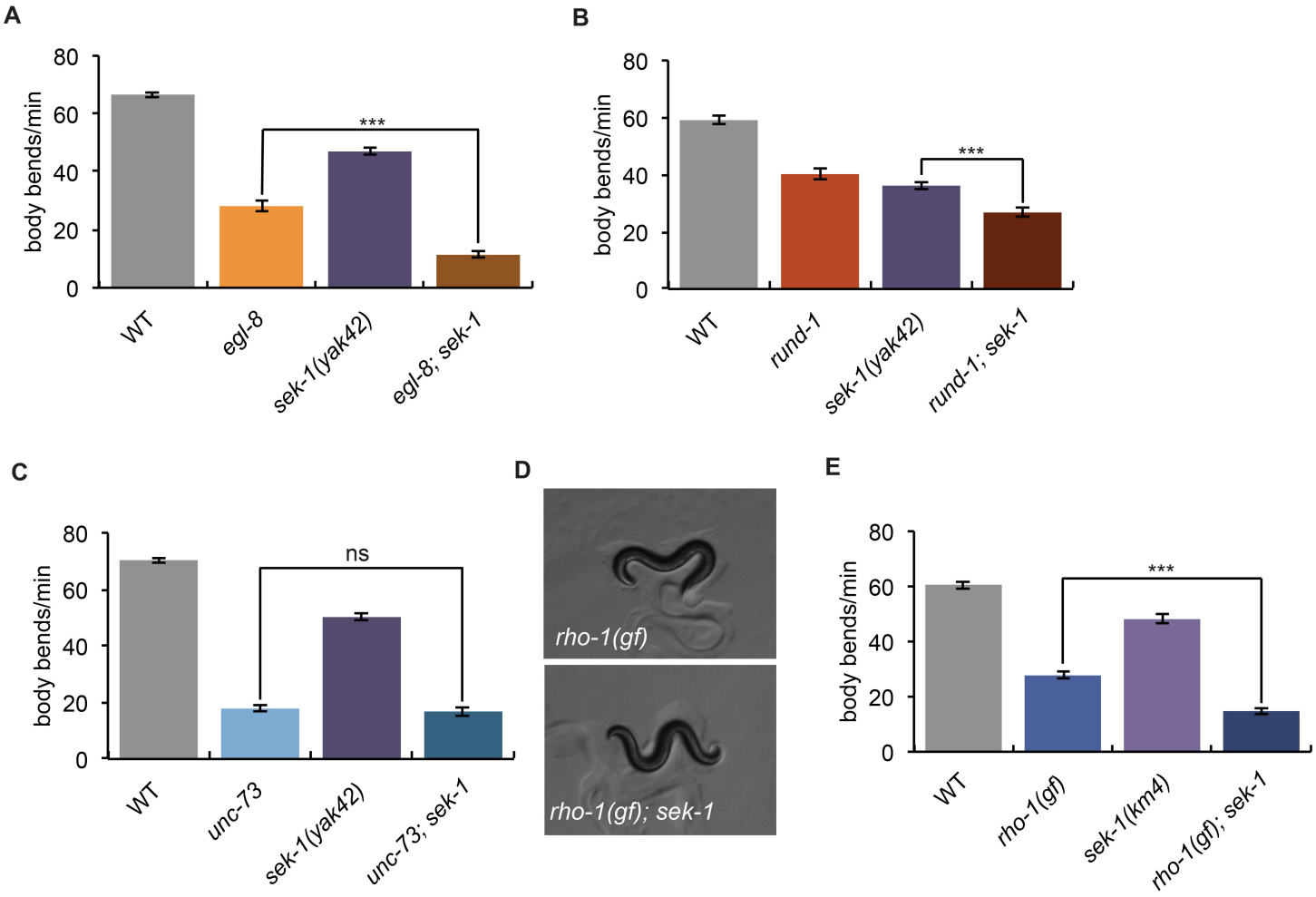

bioRxiv preprint doi: https://doi.org/10.1101/093252; this version posted December 13, 2016. The copyright holder for this preprint (which was not certified by peer review) is the author/funder, who has granted bioRxiv a license to display the preprint in perpetuity. It is made available under aCC-BY-NC 4.0 International license.
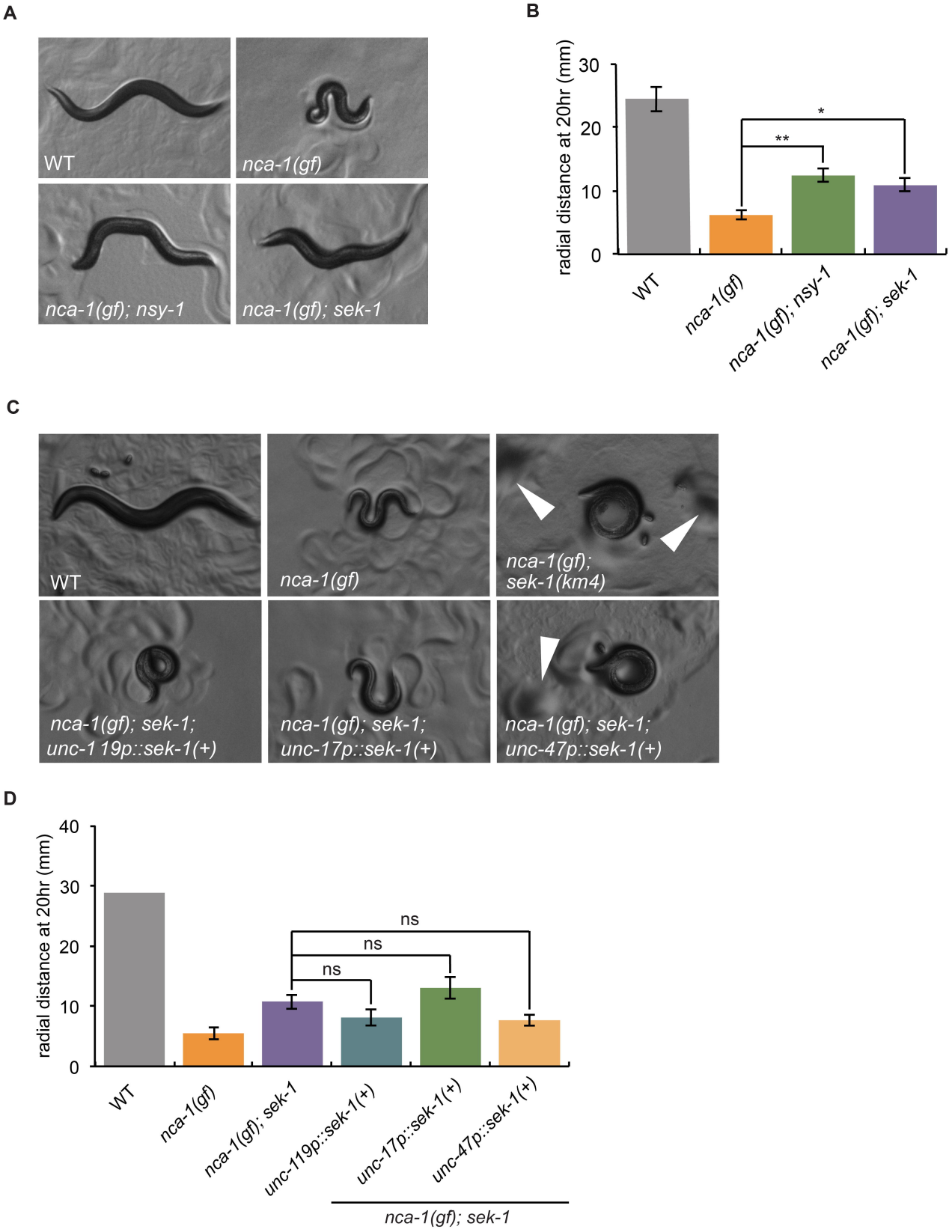
Figure 5